JCTC Journal of Chemical Theory and Computation

Article

pubs.acs.org/JCTC

Probing the Unfolded Configurations of a β-Hairpin Using Sketch-Map

Albert Ardevol,*[,†] Gareth A. Tribello,[‡] Michele Ceriotti,[§] and Michele Parrinello[†]

[†]Computational Science, Department of Chemistry and Applied Biosciences, ETH Zurich, USI-Campus, Via Giuseppe Buffi 13, C-6900 Lugano, Switzerland

[‡]Atomistic Simulation Centre, School of Mathematics and Physics, Queen's University Belfast, Belfast BT7 1NN, United Kingdom

[§]Laboratory of Computational Science and Modelling, EPFL, CH-1015 Lausanne, Switzerland

Supporting Information

ABSTRACT: This work examines the conformational ensemble involved in β-hairpin folding by means of advanced molecular dynamics simulations and dimensionality reduction. A fully atomistic description of the protein and the surrounding solvent molecules is used, and this complex energy landscape is sampled by means of parallel tempering metadynamics simulations. The ensemble of configurations explored is analyzed using the recently proposed sketch-map algorithm. Further simulations allow us to probe how mutations affect the structures adopted by this protein. We find that many of the configurations adopted by a mutant are the same as those adopted by the wild-type protein. Furthermore, certain mutations destabilize secondary-structure-containing configurations by preventing the formation of hydrogen bonds or by promoting the formation of new intramolecular contacts. Our analysis demonstrates that machine-learning techniques can be used to study the energy landscapes of complex molecules and that the visualizations that are generated in this way provide a natural basis for examining how the stabilities of particular configurations of the molecule are affected by factors such as temperature or structural mutations.

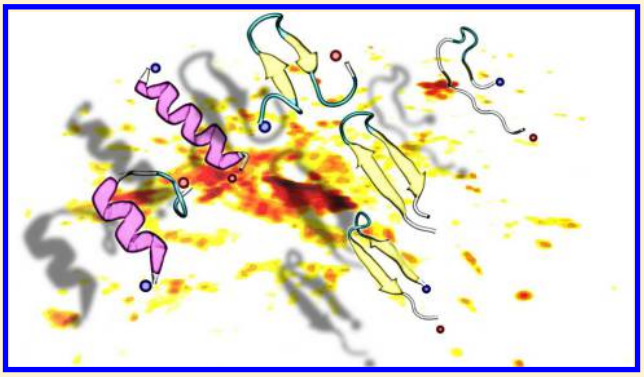

1. INTRODUCTION

Protein molecules are the workhorses of the cell and are responsible for biological functions ranging from enzymatic catalysis to cell motility.[1] In many proteins, this functionality is connected to the fact that the protein adopts a very specific tertiary structure, and in much of biochemistry, a protein's function and behavior in the cell is rationalized by referring to specific details in the protein's static, tertiary structure. Although this approach has been very successful, there is a growing consensus that this static picture of protein function is often incomplete. Processes such as signaling[2] and allosteric binding[3] as well as the growing class of so-called intrinsically disordered proteins[4] all suggest that the dynamical behavior of proteins is important and that this must be incorporated when considering protein function.

This requirement to understand both the average (static) structure of the protein and its dynamical behavior presents particular problems to the experimentalist. The first concerns how to extract time-resolved structural information, as opposed to time-averaged information, from experiments. Simulations help enormously in this regard by providing tools that allow one to "watch" protein motions in real time.[5] That said, explicit all-atom simulations of proteins provide almost too much information. In a typical molecular dynamics (MD) simulation, the changes in the positions of all of the atoms in the protein as a function of time are calculated. The trajectory that is output when a system of N atoms is simulated thus consists of an ordered set of $3N$-dimensional vectors. The problem then, when analyzing the trajectory, is that the information on the interesting long-time scale events (e.g., protein folding or conformational changes) is hidden in a sea of information on what are, for the most part, uninteresting, short-time scale events (e.g., bond vibrations). What we would really like to do is to obtain a representation of the trajectory that is based on a small number of variables, which differentiate between structures that interconvert on the time scale of interest. Any remaining variables are those that differentiate between structures that interconvert more rapidly; these can be safely integrated out.

A second difficulty that arises with theories that incorporate the dynamical behavior of the protein as well as its static structure concerns the explanation of mutagenesis data. When a protein's mode of operation can be rationalized based only on the averaged tertiary structure, it is easy to visualize, and hence understand, how mutations affect structure and hence functionality.[6] By contrast, if the dynamical behavior is important, it becomes far more difficult to explain why the

Received: October 24, 2014
Published: February 10, 2015

DOI: 10.1021/ct500950z
J. Chem. Theory Comput. 2015, 11, 1086−1093

functionality changes upon mutation. The average structures of the mutant and wild type could now be the same, and any differences in functionality might arise only because the mutant subtly perturbs the energy landscape and makes it more/less favorable for the protein to adopt some special, higher-energy, biological active form.[7] Atomistic simulations can again play a role when it comes to phenomena such as these. In addition, the question to be addressed in such simulations is articulated more clearly. We simply have to find whether there are particular configurations of the protein that have free energies that are comparable with the free energy of the folded state for the wild type and determine how the free energies of these structures relative to the folded state are affected by the mutation.

In this article, we show one way that simulation can address this question of how a mutation affects protein function. The essence of our approach is to use long parallel tempering metadynamics[8] simulations to explore the part of configuration space that is energetically accessible both to the wild type and mutant. Parallel tempering methods have been extensively used to enhance sampling in simulations of small peptides[9−11] because peptides tend to have a relatively low melting temperature and because they tend to have fast conformational diffusion in the unfolded ensemble. Parallel tempering has been shown to perform well for systems with these characteristics.[12] The output from these simulations is high-dimensional and difficult to interpret, which we resolve by using the sketch-map algorithm[13] to generate a two-dimensional map of configuration space. Free energy surfaces as a function of these coordinates give insight into the likelihood of the protein adopting a particular configuration. As such, differences in the behavior of the mutant and wild-type sequences can be understood by comparing the free energy surfaces obtained from the simulations of the wild type and the mutant.

2. BACKGROUND

There are a number of nonlinear dimensionality reduction (NLDR) algorithms[14−18] that are now used almost routinely to generate low-dimensionality representations of more high-dimensional information. In these algorithms, a computer is used to fit the parameters of some nonlinear function, which transforms the high-dimensional coordinates to a lower-dimensional vector. When using any dimensionality reduction algorithm, and in particular when choosing the particular nonlinear function to fit, one is forced to make assumptions about the structure of the high-dimensional data. As a consequence, some of these algorithms may not necessarily be well-suited for treating the sort of data one extracts from a typical molecular dynamics (MD) or enhanced sampling trajectory. The sketch-map dimensionality reduction algorithm[13,19] was developed with the features of the configurational landscape of atomic and molecular systems that perhaps make using these other algorithms problematic in mind. In particular, sketch-map disregards the information that corresponds to thermal fluctuations around a (meta)stable structure. This is achieved by doing a form of multidimensional scaling (MDS)[20] in which projections for a set of N high-dimensionality, landmark points are found by minimizing the following stress function

$$\begin{aligned} \chi^2 &= \sum_{i\neq j} [F(R_{ij}) - f(r_{ij})]^2 \\ \text{where} \quad f(r) &= 1 - (1 + (2^{a/b} - 1)(r/\sigma)^a)^{-b/a} \\ \text{and} \quad F(R) &= 1 - (1 + (2^{A/B} - 1)(R/\sigma)^A)^{-B/A} \end{aligned} \tag{1}$$

where R_{ij} is the dissimilarity between landmark points $\mathbf{X}_i$ and $\mathbf{X}_j$ and r_{ij} is the distance between their projections $\mathbf{x}_i$ and $\mathbf{x}_j$. In this work, we have measured dissimilarities between protein configurations by measuring how much the full set of protein backbone dihedral angles changes on moving between the two configurations. We tune the values of the parameters in the sigmoid functions, $F(R)$ and $f(r)$, using the methods described in the appendices of our previous work.[21] The form of these sigmoid functions ensures that close together points, which are most likely in the same basin, are then projected close together, whereas points that are far apart, and are thus likely to be in basins that are not connected by a single transition state, are projected far apart. Furthermore, by selecting different a parameters for the high-dimensional and low-dimensional sigmoid functions, $F(R_{ij})$ and $f(r_{ij})$, respectively, one can alleviate the problems that arise when attempts are made to project the high-dimensionality features that are present in the basins in the low-dimensionality space.[21]

Histograms, and free energy surfaces, can be constructed as a function of sketch-map coordinates because, once projections of the initial landmark frames have been determined, the projection, $\mathbf{x}$, of any point in the high-dimensionality space, $\mathbf{X}$, can be found by minimizing

$$\delta^2(\mathbf{x}) = \sum_{i=1}^{N} \{F[R_i(\mathbf{X})] - f[r_i(\mathbf{x})]\}^2 \tag{2}$$

where $R_i(\mathbf{X})$ is the dissimilarity between $\mathbf{X}$ and the ith landmark point and $r_i(\mathbf{x})$ is the distance between point $\mathbf{x}$ and the projection of the ith landmark. In a recent paper,[21] we showed that this procedure is remarkably robust. In particular, we found that we could use sketch-map coordinates constructed using N landmark frames to project configurations that were markedly different from all of the landmarks. Furthermore, if the two configurations being projected were also markedly different from each other, then they would be projected at two well-separated locations in the sketch-map plane. In other words, sketch-map coordinates can differentiate between distinct structures even if these configurations are not represented in the set of landmarks. This feature is crucial in this work, as it gives us the confidence that coordinates constructed for the wild type can be used to understand the configurations adopted by a mutant. This mutant may well adopt configurations that are energetically inaccessible to the wild type and that are thus not represented in the set of landmark frames.

3. RESULTS

3.1. Simulations of Wild-Type Protein. In this study, we have examined the 16-residue C-terminal fragment of the immunoglobulin binding domain B1 of protein G of Streptococcus protein in explicit solvent (amino acids sequence Ace-GEWTYDDATKTFTVTE-NMe).[22−24] We used Gromacs-4.5.5[25] and the variant on replica exchange discussed by Deighan et al.[11] In this protocol, a 100 ns parallel tempering well-tempered ensemble metadynamics[26] simulation was run with 32 replicas that had temperatures distributed between 268

DOI: 10.1021/ct500950z
J. Chem. Theory Comput. 2015, 11, 1086−1093

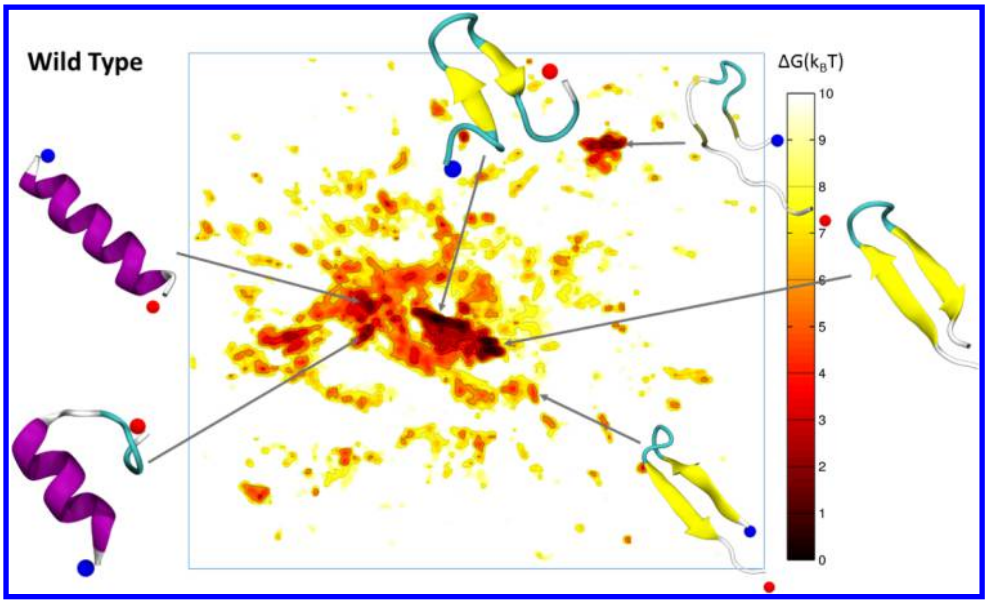

Figure 1. Free energy surface at 299 K for the wild type of the β-hairpin protein as a function of the sketch-map coordinates. The small inset figures show representative structures from each of the minima.

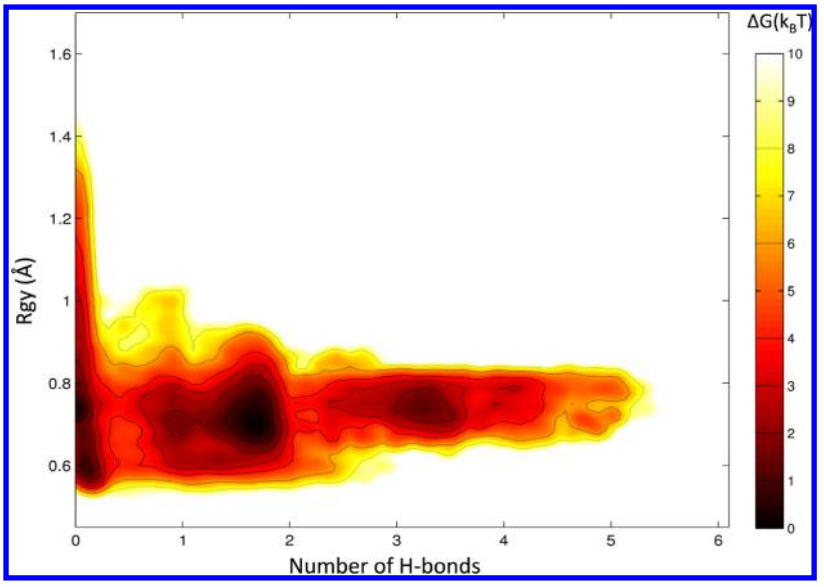

Figure 2. Free energy surface for the wild-type protein studied in this work as a function of the number of hydrogen bonds that should be present in the folded configuration and the radius of gyration. The folded state is projected on the right-hand side, misfolded β hairpin configurations appear in the center, and all other configurations, including α-helical ones, are projected on the left-hand side near the y-axis.

and 625 K. In this first set of simulations, a history-dependent bias is added that is a function of the potential energy of the system. Biases as a function of this collective variable have been shown to enhance the fluctuations in the energy.[27] As such, using this form of biasing in tandem with parallel tempering allows one to lower the number of replicas required while ensuring that the exchange probabilities remain reasonable. Once these simulations were completed, we ran 300 ns/replica long well-tempered metadynamics parallel tempering simulations. In these calculations, the bias on the potential was kept constant and further metadynamics biases were added on the radius of gyration and the number of hydrogen bonds between backbone atoms. All metadynamics calculations were run using PLUMED 1.3,[28,29] and input files are provided in the Supporting Information.

Sketch-map coordinates were generated by selecting 1000 landmark points from our wild-type trajectory using the staged algorithm[21] with gamma equal 0.1 and wgamma equal to 1. The set of Ramachandran angles for each protein configuration was used for the high-dimensional, **X** vectors in eqs 1 and 2 rather than the position of all of the atoms because by doing so we eliminate a large amount of redundant information while still providing a good description of the variability in protein structure. Optimal two-dimensional projections for each of the landmark protein configurations were found by minimizing eq 1 with $\sigma = 6$, $A = 8$, $B = 8$, $a = 2$, and $b = 8$ using the optimization algorithm described in ref 13. Then, once this initial set of projections was found, the remainder of the trajectory was projected into the sketch-map space using eq 2. The free energy surface of the replica at 299.1 K shown in

DOI: 10.1021/ct500950z
J. Chem. Theory Comput. 2015, 11, 1086−1093

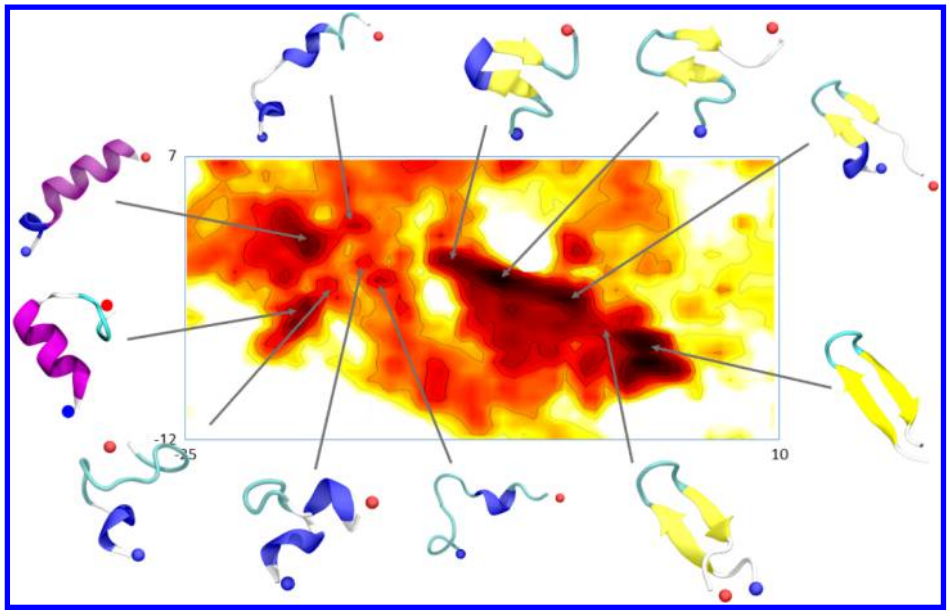

Figure 3. Figure showing the region of the sketch-map projection of the free energy surface containing the β hairpin and α-helical configurations. Representative configurations for each of the minima in this region are shown.

Figure 1 was then constructed by reweighting the histogram generated from our parallel tempering well-tempered metadynamics simulations using the method described in ref 30. There are a number of notable features in Figure 1. First, this figure shows that the free energy surface for the protein is very rough. There are many basins, and each of these basins corresponds to a markedly different protein configuration. This behavior should be compared with that observed in the free energy surface shown in Figure 2, in which the free energy is shown as a function of the radius of gyration and the degree to which the hydrogen bonds that would form in the β hairpin have formed. Importantly, the coordinate used to measure hydrogen bonding in Figure 2 is different from that used in the metadynamics simulations. In the metadynamics, our measure of the number of backbone hydrogen bonds is agnostic and simply counts the total number that have been formed. By contrast, for easy comparison with previous literature,[8,31,32] in this figure we count only those hydrogen bonds that would be present in the final, folded β-hairpin configuration.

Figure 2 shows a free energy surface that is considerably smoother than that shown in Figure 1. One now sees only three distinct minima in the free energy landscape, and many of the basins that were visible in Figure 1 appear to have disappeared. It is therefore apparent that when these commonly used collective variables are used to analyze the dynamics of the protein one can only really make judgements about the relative stabilities of the folded (β-hairpin) structure and the unfolded state. However, Figure 1 shows us that multiple configurations, and perhaps more pertinently multiple energetic basins, make up this unfolded state. There is incomplete agreement in the literature about what structures together comprise the unfolded ensemble for this protein. While some simulation studies suggest that there is no significant α-helical content,[32] others see a substantial number of helical configurations.[33−35] The free energy surface in Figure 1 seems to suggest that α-helical configurations are present and that they have free energies that are comparable with those of the β hairpin.

Another contentious issue in the literature on this protein concerns the various misfolded configurations that the protein can adopt. Bonomi et al.[36] suggested the existence of one misfolded state. Meanwhile, Best et al.[35] found multiple misfolded configurations, which included Bonomi's. In our free energy surface, we see many of the misfolded configurations that were observed in these studies. We do not see all because different force fields, which perhaps stabilize different configurations, were used in these other studies. In our work, we used AMBER99SB-ILDN*[37] because it has been shown to reproduce experimental observations for small peptides and proteins well.[38]

Figure 3 shows the region of the sketch-map free energy surface around the α helical and β hairpin minima in more detail. This figure shows clearly that there are many minima in the free energy landscape in this region corresponding to structures with various degrees of α-helical and β-sheet-like character. The most stable configuration is the folded β hairpin. However, there are a number of partially folded hairpins that lie relatively close in energy. These configurations have a free energy that is only slightly lower than that of a perfect α helix. Most importantly, however, a comparison between Figures 1 and 2 clearly shows that variables such as the radius of gyration or the number of native hydrogen bonds, which measure the degree to which the structure resembles that in the folded state, give an incomplete picture of the unfolded state. α-Helical configurations appear in a separate basin from the misfolded configurations in Figure 1 but are combined in a single basin in Figure 2.

It is tempting to look for the transition pathways between configurations in these sketch-map coordinates. Care should be taken when doing so, however, as first no dynamical information was used in the construction of these coordinates. At best, structures appear close together in the projection because they are relatively close together in the high-dimensional space. This does not necessarily mean that the system will rapidly interconvert between these configurations: two structures that appear close together may well be separated by a substantial energy barrier. Second, we have shown[19] that continuous paths in the high-dimensional space can appear to be discontinuous when projected using sketch-map.

DOI: 10.1021/ct500950z
J. Chem. Theory Comput. 2015, 11, 1086−1093

Plotting the free energy surface as a function of the sketch-map variables at a variety of different temperatures using a single reference map obtained at an intermediate temperature is an interesting exercise. When this is done for the trajectories in this work, we observe results that are similar to those obtained in a recent work on Lennard-Jones clusters.[21] Figure 4 shows

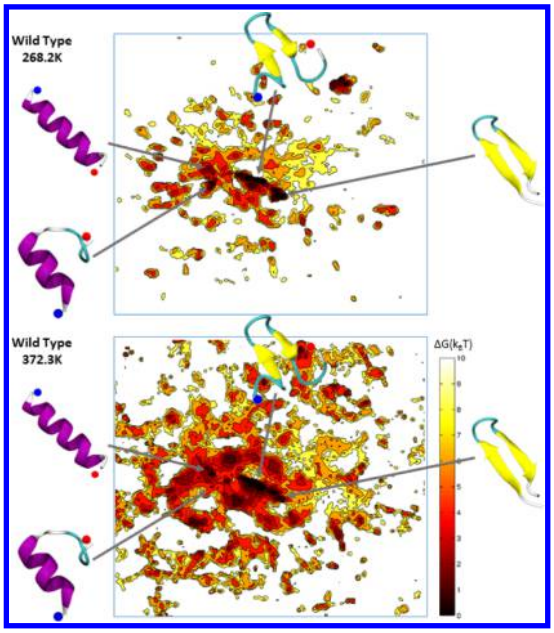

Figure 4. Free energy surfaces for the wild-type protein examined in this work as a function of the sketch-map coordinates at temperatures of 268.2 and 372.3 K. These surfaces were generated by projecting the trajectories for the replicas at these temperatures using a set of landmarks extracted from the trajectory at 299.2 K. As such, the various basins in these landscapes can be compared directly with those in Figure 1. The figure shows that at low temperatures the system explores a small part of configuration space and is largely confined to the folded states. At higher temperatures, the system explores more of configuration space including a wide variety of unfolded structures. However, this free energy surface tells us that the system will spend a considerable portion of its time in folded configurations even at these relatively high temperatures.

that at low temperatures the system is confined to the low-energy folded states: the α-helical and β-sheet configurations. By contrast, at higher temperatures, the system is free to explore a much wider portion of configuration space including many high-energy configurations. It is interesting to note that basins corresponding to the hairpin, the mis-folded hairpin, and the helix are present at all temperatures. In other words, the system spends a substantial amount of time in folded states even when it is at a temperature of 373 K. The apparent stabilities of these folded configurations can be rationalized by noting that the basins corresponding to each of them are wider in the higher temperature free energy surface. It would seem then that increases in entropy that occur because the system fluctuates more wildly about the equilibrium structures at higher temperatures serve to stabilize the folded structure even when the temperature is high. This should be contrasted with the case of small clusters,[21] where the enthalpic minima appear to be very rigid. In these systems, structural fluctuations about low-energy minima do not appear to increase strongly with temperature. Consequently, the weights of the enthalpic basins become completely irrelevant when the temperature is raised.

3.2. Trpzip4 and D46A Mutations. It has been suggested that protein energy landscapes always have minima corresponding to the various secondary structural elements because these features in the energy landscape emerge as a result of interactions between the backbone atoms that are unaffected by the amino acid sequence.[39,40] In this view, the amino acid sequence only perturbs the energies of this universal library of secondary structure motifs. As a result, the sequence, rather than controlling the shape of the funnel that leads to the folded state,[40] serves only to select a folded state from a smörgåsbord of allowable protein configurations. The sketch-map coordinates discussed in the previous section provide us with an interesting opportunity to examine this kind of hypothesis. By projecting the free energy surface for a mutant protein using the sketch-map coordinates that we generated in the previous section for the wild-type protein, we can do a basin-by-basin comparison of the free energy landscapes for two proteins with different amino acid sequences. In other words, we can examine how the free energy for each of the individual basins in the energy landscape is perturbed by the mutation and can thus perhaps provide more detailed insight than observing simply that one mutation stabilizes the folded state while the other destabilizes it.

With the above experiment in mind, we ran parallel tempering well-tempered metadynamics simulations similar to those described at the start of the previous section on two mutations of the β-hairpin protein. In the first of these mutants, we changed the tyrosine, phenylalanine, and valine groups on residues 45, 52, and 54 to tryptophans. The residues we mutated are shown in blue in the left panel of Figure 5. This

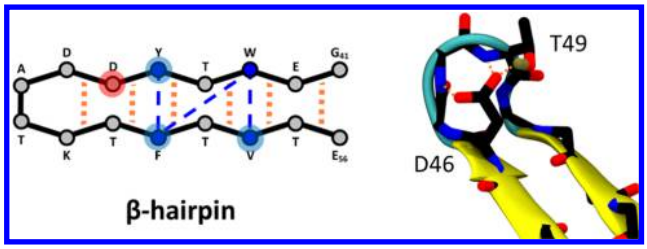

Figure 5. Figure illustrating the mutations studied in this work. The left panel shows a schematic of the folded configuration. The red dashed lines indicate the various hydrogen bonds that form between backbone groups in the folded state, and the blue dashed lines illustrate the favorable hydrophobic interactions that serve to stabilize the folded state. In the first mutation, we examined a mutant in which the residues highlighted in blue were changed to tryptophans. In the second mutation, the aspartate residue highlighted in red was changed to an alanine. As shown in the right panel of the figure, this aspartate (D46) forms a hydrogen bond to residue T49 in the wild type, which serves to stabilize the loop region for the folded β hairpin. Alanine cannot form this hydrogen bond and thus this mutation destabilizes the folded state.

figure shows that the mutated residues participate in a number of hydrophobic interactions that stabilize the core of the structure. Hence, by making these already hydrophobic residues even more hydrophobic, we would expect to further stabilize the folded β-hairpin configuration,[41,42] which is precisely what is observed in Figure 6. The minima corresponding to the β-hairpin configuration becomes deeper, as do the satellite basins around it that correspond to the various partially unfolded configurations of this structure.

DOI: 10.1021/ct500950z
J. Chem. Theory Comput. 2015, 11, 1086−1093

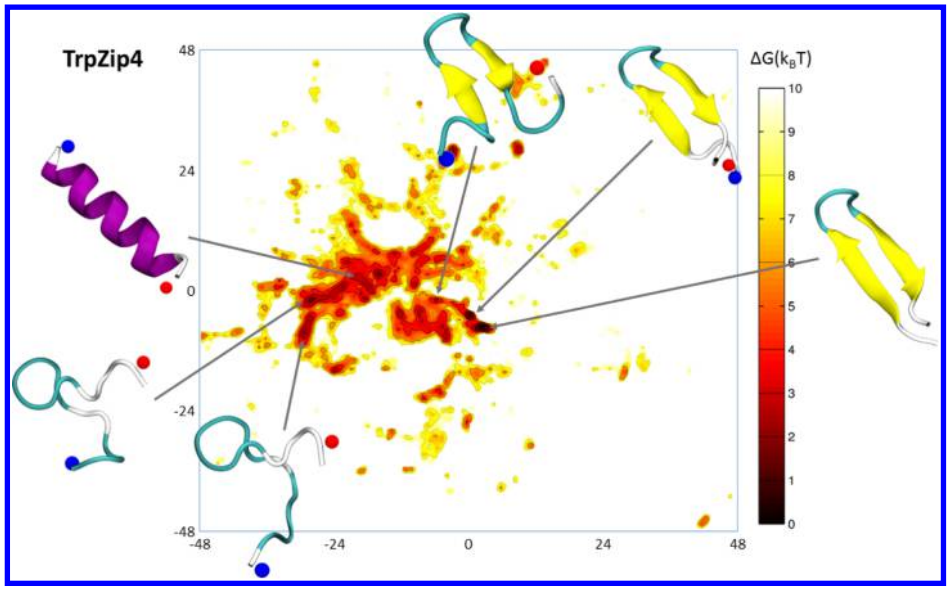

Figure 6. Free energy surface at 299 K for a mutant protein in which residues 45, 52, and 54 have been changed to tryptophans. By comparing this landscape with that of the wild type in Figure 1, it becomes apparent that this mutation serves to stabilize the folded β-hairpin configuration.

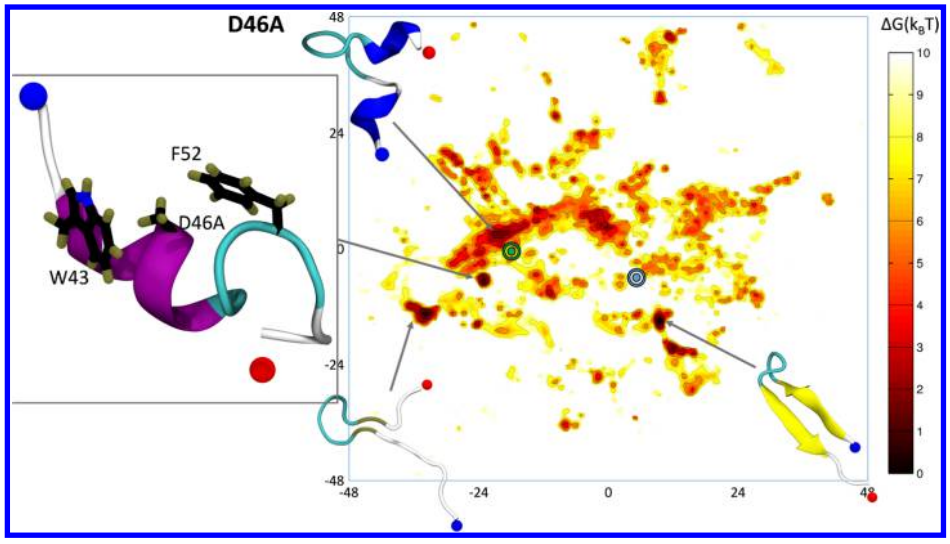

Figure 7. Free energy surface at 299 K for a mutant protein in which residue 46 has been changed into an alanine. The blue and the green markers indicate where the folded and the linear α-helical configurations are projected in the free energy surface of the wild type. By comparing this landscape with that of the wild type in Figure 1, it becomes apparent that this mutation serves to destabilize the folded β-hairpin configuration as well as the linear α helix. As discussed in the text, we see from our simulation that the alanine on residue 46, as well as not forming the hydrogen bonds that stabilize the β hairpin, can also form the hydrophobic contacts shown in the left panel of this figure. This serves to destabilize the linear α helix.

Figure 6 shows that the free energy difference between the perfect α-helix structure and the folded β hairpin is larger for this mutated protein than it is in the wild type. Even so, the α helix still has a reasonably low free energy, so the system would still be expected to spend a considerable fraction of its time in α-helical configurations. The reason for this is probably connected to the fact that α helices are held together by backbone hydrogen bonds between carboxylate and amine groups that are four residues apart on the protein chain. A mutation of the protein would not be expected to change the strength of these particular interactions significantly. A significant change in the hydrophobicity of the amino acid side chains might, by contrast, act to destabilize the α helix because, in an α helix, all of the side chains are exposed to the solvent. It would seem from Figure 6, however, that making hydrophobic residues slightly more hydrophobic does not perturb the free energy landscape greatly enough to bring about this change.

In the second mutation, we substituted the aspartate on position 46, which is shown in red in the left panel of Figure 5, for an alanine. As shown in the right panel of Figure 5, in the wild-type this aspartate stabilizes the loop region of the folded state by forming hydrogen bonds both to the backbone amide nitrogens of those residues in the loop and to the side chain of threonine 49. Alanine will not form these hydrogen bonds, which explains why there is no longer a basin corresponding to the β-hairpin structure or any satellite basins corresponding to partially unfolded β hairpins in the free energy landscape for this mutant (Figure 7). Interestingly, this mutation also appears to affect the stability of the perfect α helix. The linear α-helical configuration that appears in Figures 1 and 6 is not shown in Figure 7 because the system did not visit this particular

DOI: 10.1021/ct500950z
J. Chem. Theory Comput. 2015, 11, 1086−1093

configuration in our parallel tempering simulations on the D46A mutant. This fact is evidenced in the free energy surfaces shown in Figures 1, 6, and 7. In the first two of these free energy surfaces, the linear α helix is shown to correspond to a rather distinctive sausage-shaped basin in the free energy landscape, which is no longer visible in Figure 7. To be clear, it is not that this mutant does not visit α helices at all, rather it is that the α-helical configurations that it does visit are folded back on themselves (see the left panel of Figure 7). One explanation for this is that by substituting the aspartate on residue 46 with an alanine we have made a formerly hydrophilic residue hydrophobic. As discussed previously, this would destabilize the α helix, as in this configuration all of the side chains are exposed to the solvent. In addition, the left panel of Figure 7 show that this mutated alanine group forms two hydrophobic contacts that stabilize a bent α helix over the linear one.

As discussed previously, the global minimum for both the wild type and the TrpZip4 mutant is a β-hairpin configuration. There is no basin corresponding to this structure in the D46A free energy surface for the reasons discussed in the previous paragraph. However, this is not to say that β hairpins do not form for this particular amino acid sequence. There is a prominent basin that corresponds to a structure in which an antiparallel β hairpin has formed and in which the loop is between residues 44 and 47 in the bottom right-hand corner of the free energy surface shown in Figure 7. This structure is favorable because within it there are numerous hydrophobic contacts. Furthermore, it appears in the free energy landscapes for both the wild type and TrpZip4 mutant. However, in those proteins, the feature in the free energy landscape corresponding to this structure is considerably less prominent because this structure contains fewer hydrophobic contacts than the perfect β hairpin. The reason it is so prominent for D46A is almost certainly connected to the fact that it is unfavorable to form the loop between residues 47 and 51 because the (mutated) alanine group on residue 46 cannot form the prerequisite hydrogen bonds.

4. CONCLUSION

The sketch-map coordinates that have been used to analyze the long MD trajectories generated in this study have shown themselves to be a useful tool. When the free energy surface is displayed as a function of these bespoke coordinates, one can see the wide range of configurations adopted by a particular chemical system. For proteins, this means that one can use sketch-map coordinates to view, basin-by-basin, how a change in the conditions or a change in the amino acid sequence affects the free energy landscape of a protein. This is useful, as evidence keeps emerging that denaturants such as urea[31] work by changing the relative free energy of unfolded configurations. Similarly, a better understanding of how the free energy landscapes of proteins change in response to experimental conditions will allow us to better understand phenomena such as the Hoffmeister series[43] or even how changing the force field parameters changes the way phase space is sampled. Lastly, there is increasing evidence that so-called intrinsically disordered proteins play an important role in biology. Many of these proteins undergo folding and binding at the same time and hence untangling their modus operandi requires a detailed view on how free energies of folding are perturbed by binding and vice versa.

Our results suggest that mutations can stabilize or destabilize particular configurations of the peptide by either allowing it to form new energetically favorable contacts or by preventing them from forming particular native contacts. It seems reasonable to suppose that this may well be valid for other small, isolated proteins, so our results would appear to support backbone theories[39,40] of protein folding more than they support those theories based on the amino acids sequence sculpting the folding funnel.[44] However, in a bigger protein, regions of secondary structure are likely to be stabilized by additional interactions that will all serve to ensure that the protein adopts its biologically active, tertiary structure. In these proteins, the tertiary structure is thus less likely to be affected by small (point) mutations. As such, further study is thus certainly required if we are to determine the effect mutations have on the folding landscape in general terms.

We were able to come to these conclusions because sketch-map coordinates allow one to perform an unbiased analysis of the simulation results. Additionally, eq 2 ensures that we can calculate projections easily for any vector of 30 torsional angles. We can even use these coordinates to enhance sampling and to thus drive the system to explore high-energy parts of configuration space.[19] All of the evidence that we have accumulated thus far further suggests that this procedure will produce sensible projections. We thus have coordinates that can be used for a number of different amino acid sequences and that are not constructed based on previous knowledge on the structure of the folded state. In short, we are in a position where we can compare data collected from multiple trajectories and where our previous understanding does not limit our analysis. As such, there is thus a greater chance of discovering unexpected or surprising results.

■ ASSOCIATED CONTENT

Supporting Information

PLUMED 1.3 input files used for the metadynamics simulations. This material is available free of charge via the Internet at http://pubs.acs.org.

■ AUTHOR INFORMATION

Corresponding Author

*E-mail: albert.ardevol@phys.chem.ethz.ch.

Funding

The authors acknowledge funding from the European Union (grant ERC-2009-AdG-24707). A.A. was supported by an EMBO long-term fellowship.

Notes

The authors declare no competing financial interest.

■ ACKNOWLEDGMENTS

The authors would like to thank CSCS for computer time.

■ REFERENCES

(1) Lodish, H.; Berk, A.; Matsudaira, P.; Kaiser, C. A.; Krieger, M.; Scott, M. P.; Zipursky, S. L.; Darnell, J. *Molecular Cell Biology*, 5th ed.; W. H. Freeman: New York, 2003.

(2) Dunker, A. K.; Silman, I.; Uversky, V. N.; Sussman, J. L. *Curr. Opin. Struct. Biol.* **2008**, *18*, 756−764.

(3) Christopoulos, A. *Nat. Rev. Drug Discovery* **2002**, *1*, 198−210.

(4) Dyson, H. J.; Wright, P. E. *Nat. Rev. Mol. Cell Biol.* **2005**, *6*, 197−208.

DOI: 10.1021/ct500950z
J. Chem. Theory Comput. 2015, 11, 1086−1093

(5) Shaw, D. E.; Maragakis, P.; Lindorff-Larsen, K.; Piana, S.; Dror, R. O.; Eastwood, M. P.; Bank, J. A.; Jumper, J. M.; Salmon, J. K.; Shan, Y.; Wriggers, W. *Science* **2010**, *330*, 341−346.
(6) Li, Y.; Cirino, P. C. *Biotechnol. Bioeng.* **2014**, *111*, 1273−1287.
(7) Bouvignies, G.; Vallurupalli, P.; Hansen, D. F.; Correia, B. E.; Lange, O.; Bah, A.; Vernon, R. M.; Dahlquist, F. W.; Baker, D.; Kay, L. E. *Nature* **2011**, *477*, 111−134.
(8) Bussi, G.; Gervasio, F. L.; Laio, A.; Parrinello, M. *J. Chem. Am. Soc.* **2006**, *128*, 13435−13441.
(9) Gnanakaran, S.; Nymeyer, H.; Portman, J.; Sanbonmatsu, K. Y.; Garca, A. E. *Curr. Opin. Struct. Biol.* **2003**, *13*, 168−174.
(10) Weinstock, D. S.; Narayanan, C.; Felts, A. K.; Andrec, M.; Levy, R. M.; Wu, K.-P.; Baum, J. *J. Am. Chem. Soc.* **2007**, *129*, 4858−4859.
(11) Deighan, M.; Bonomi, M.; Pfaendtner, J. *J. Chem. Theory Comput.* **2012**, *8*, 2189−2192.
(12) Zuckerman, D. M. *Annu. Rev. Biophys.* **2011**, *40*, 41−62.
(13) Ceriotti, M.; Tribello, G. A.; Parrinello, M. *Proc. Natl. Acad. Sci. U.S.A.* **2011**, *108*, 13023−13029.
(14) Tenenbaum, J. B.; Silva, V. d.; Langford, J. C. *Science* **2000**, *290*, 2319−2323.
(15) Roweis, S. T.; Saul, L. K. *Science* **2000**, *290*, 2323−2326.
(16) Coifman, R. R.; Lafon, S.; Lee, A. B.; Maggioni, M.; Nadler, B.; Warner, F.; Zucker, S. W. *Proc. Natl. Acad. Sci. U.S.A.* **2005**, *102*, 7432−7437.
(17) Coifman, R. R.; Lafon, S. *Appl. Comput. Harmonic Anal.* **2006**, *21*, 5−30.
(18) Belkin, M.; Niyogi, P. *Neural Comput.* **2003**, *15*, 1373−1396.
(19) Tribello, G. A.; Ceriotti, M.; Parrinello, M. *Proc. Natl. Acad. Sci. U.S.A.* **2012**, *109*, 5196−5201.
(20) Cox, T. F.; Cox, M. A. A. *Multidimensional Scaling*; Chapman and Hall: London, 1994.
(21) Ceriotti, M.; Tribello, G. A.; Parrinello, M. *J. Chem. Theory Comput.* **2013**, *9*, 1521−1532.
(22) Blanco, F. J.; Rivas, G.; Serrano, L. *Nat. Struct. Biol.* **1994**, *1*, 584−590.
(23) Hughes, R.; Waters, M. *Curr. Opin. Struct. Biol.* **2006**, *16*, 514−524.
(24) Muñoz, V.; Thompson, P.; Hofrichter, J.; Easton, W. *Nature* **1997**, *390*, 196−199.
(25) Hess, B.; Kutzner, C.; van der Spoel, D.; Lindahl, E. *J. Chem. Theory Comput.* **2008**, *4*, 435−447.
(26) Laio, A.; Parrinello, M. *Proc. Natl. Acad. Sci. U.S.A.* **2002**, *99*, 12562−12566.
(27) Bonomi, M.; Parrinello, M. *Phys. Rev. Lett.* **2010**, *104*, 190601.
(28) Bonomi, M.; Branduardi, D.; Bussi, G.; Camilloni, C.; Provasi, D.; Raiteri, P.; Donadio, D.; Marinelli, F.; Pietrucci, F.; Broglia, R. A.; Parrinello, M. *Comput. Phys. Commun.* **2009**, *180*, 1961−1972.
(29) Tribello, G. A.; Bonomi, M.; Branduardi, D.; Camilloni, C.; Bussi, G. *Comput. Phys. Commun.* **2014**, *185*, 604−613.
(30) Bonomi, M.; Barducci, A.; Parrinello, M. *J. Comput. Chem.* **2009**, *30*, 1615−1621.
(31) Berteotti, A.; Barducci, A.; Parrinello, M. *J. Am. Chem. Soc.* **2011**, *133*, 17200−17206.
(32) Zhou, R.; Berne, B.; Germain, R. *Proc. Natl. Acad. Sci. U.S.A.* **2001**, *98*, 14931−14936.
(33) Best, R. B.; Mittal, J. *Proc. Natl. Acad. Sci. U.S.A.* **2011**, *108*, 11087−11092.
(34) Garcia, A.; Sanbonmatsu, K. *Proteins: Struct., Funct., Genet.* **2001**, *42*, 345−354.
(35) de Sancho, D.; Mittal, J.; Best, R. B. *J. Chem. Theory Comput.* **2013**, *9*, 1743−1753.
(36) Bonomi, M.; Branduardi, D.; Gervasio, F. L.; Parrinello, M. *J. Am. Chem. Soc.* **2008**, *130*, 13938−13944.
(37) Lindorff-Larsen, K.; Piana, S.; Palmo, K.; Maragakis, P.; Klepeis, J. L.; Dror, R. O.; Shaw, D. E. *Proteins: Struct., Funct., Bioinf.* **2010**, *78*, 1950−1958.
(38) Lindorff-Larsen, K.; Maragakis, P.; Piana, S.; Eastwood, M. P.; Dror, R. O.; Shaw, D. E. *PLoS One* **2012**, *7*, e32131.
(39) Rose, G. D.; Fleming, P. J.; Banavar, J. R.; Maritan, A. *Proc. Natl. Acad. Sci. U.S.A.* **2006**, *103*, 16623.
(40) Hegler, J. A.; Weinkam, P.; Wolynes, P. G. *HFSP J.* **2008**, *2*, 307.
(41) Noy, K.; Kalisman, N.; Keasar, C. *BMC Struct. Biol.* **2008**, *8*, 27.
(42) Juraszek, J.; Bolhuis, P. G. *J. Phys. Chem. B* **2009**, *113*, 16184−16196.
(43) Hofmeister, F. *Arch. Exp. Pathol. Pharmacol.* **1888**, *24*, 247−260.
(44) Oliverberg, M.; Wolynes, P. G. *Q. Rev. Biophys.* **2008**, *71*, 245.

DOI: 10.1021/ct500950z
J. Chem. Theory Comput. 2015, 11, 1086−1093